MEaSUREs-funded project titled:
"Creating an extended and consistent ESDR of the ocean surface winds, stress and their dynamically-significant derivatives for the period 1999-2022"

User's Guide

01 December, 2022

Team members:

Svetla Hristova-Veleva [1], Bryan Stiles [1], Alexander Fore [1], Alexander Wineteer [1], David F. Moroni [1], Mark Bourassa [2], Douglas Vandemark [3], Larry O'Neill [4], Thomas Kilpatrick [5], Shakeel Asharaf [1], Ethan Wright [2], Xiaosu Xie [1], F. Joseph Turk [1], Marc Emond [3], P. Peggy Li [1], Brian Knosp [1], Quoc Vu [1], Robin Vane [1], Joseph Jacob [1], Federica Polverari [1], Philip Callahan [1], Roy S. Dunbar [1], Ernesto Rodriguez [1]

[1] - Jet Propulsion Laboratory, California Institute of Technology
[2] – Florida State University
[3] – University of New Hampshire, Durham
[4] – Oregon State University
[5] - University of California at San Diego

The research was carried out at the Jet Propulsion Laboratory, California Institute of Technology, under a contract with the National Aeronautics and Space Administration.

1. Introduction – Motivation, Goals and Objectives of the MEaSUREs project

Provided below is general information on the MEaSUREs-funded project titled: "Creating an extended and consistent Earth System Data Record (ESDR) of the ocean surface winds, stress and their dynamically-significant derivatives for the period 1999-2022".

Ocean surface winds are one of the key components of the Earth system. They are a major driver of the ocean circulation and affect the air-sea interactions, providing fuel to the weather systems by modulating the sensible and latent heat fluxes. Understanding these interactions is critical for improving weather forecasting on a variety of spatial and temporal scales – from isolated convective systems, to the organized mesoscale systems, to hurricanes, to the seasonal and intra-seasonal phenomena such as the Madden-Julian Oscillation (MJO), El Nino and the trends and variability in the large-scale atmospheric circulation (e.g. monsoon rains). Indeed, ocean surface winds and stress are Essential Climate Variables (ECV) identified by the Global Climate Observing System (GCOS) [GCOS-200, 2016].

Space-borne scatterometer observations have been used extensively for over two decades to estimate the equivalent neutral (EN) ocean surface winds. These scatterometer retrievals are of the wind vector that is relative to the ocean surface (without account for the ocean currents) and are calibrated to a 10m height above the sea level, assuming neutral stability in the process of converting surface winds to 10m winds, hereafter referred to as equivalent neutral (EN) winds. The EN winds have proved very valuable to studies of air-sea interaction (e.g. Chelton et al., 2004; O'Neill et al., 2005; Minobe et al., 2008), ocean circulation (e.g. Lovenduski and Gruber, 2005; Cunningham et al., 2007, Jiang et al., 2008), the Hadley cell (Hristova-Veleva et al., 2015) and weather phenomena, such as El Niño (Hristova-Veleva et al., 2016b) and tropical storms (e.g. Chavas and Emanuel, 2010, Hristova-Veleva et al., 2016a,c). Assimilating scatterometer winds into numerical weather prediction models has resulted in improving forecast accuracy (e.g. Isaksen and Stoffelen, 2000; Atlas et al., 2001, Marseille and Stoffelen, 2017; McCarty et al., 2018, Bhate et al., 2021). As a result of this success, operational meteorologists have grown accustomed to basing their forecast of hurricane formation and evolution on scatterometer retrievals.

Satellite scatterometer observations have been made by a number of missions over a period of more than 40 years, yet the last 23+ years (since August 1999) stand out as having a relatively continuous, near-global gap-free coverage over the ice-free oceans. ***There is a significant diversity in the instrument geometry (incidence angle), spatial resolution and the mission-specific Local-Time-of-Day (LTD) of the observations***. However, the scatterometer missions of the past 23+ years can be broadly classified in only two categories, defined by the channel-of-choice and the scanning strategy: i) the Ku-band, conically-scanning pencil beam instruments employed by NASA and the Indian Space Research Organization (ISRO); ii) the C-band, push-broom instruments employed by the European Organization for the Exploitation of Meteorological Satellites (EUMETSAT). The pencil-beam approach provides a much wider swath than the push-broom one but with higher uncertainty in the near-nadir portion of the swath. The two different measurement frequencies produce measurements that have different sensitivity to atmospheric parameters (most importantly rain) and to ocean surface parameters such as sea surface temperature (SST) and wind speed. Another factor compounding the uncertainty in the wind estimates is that different agencies use different retrieval algorithms (e.g. algorithms used by

the Royal Netherlands Meteorological Institute (KNMI) versus algorithms employed at the Jet Propulsion Laboratory (JPL), versus ISRO's algorithms, versus those adopted by the Remote Sensing Systems (RSS)), employ different Geophysical Model Functions (GMFs) to relate the scatterometer observations to the winds to be estimated, and use different ancillary data (e.g. NCEP versus ECMWF analyses/short-term forecasts) to help with the retrievals (direction estimation).

Achieving consistency between the wind vector estimates from the different scatterometers has been a long-standing goal of the IOVWST. Substational effort has gone into instrument calibration, algorithm validation and cross-evaluation, and significant progress has been made in this direction. Yet, some small but important inconsistencies still remain.

The Ocean Vector Wind (OVW) community, and the International Ocean Vector Wind Science Team (IOVWST) members (sponsored by NASA in the U.S.), in particular, are now positioned to address three issues of great importance that still face the atmospheric and oceanic users of the ocean surface vector wind satellite estimates. **To address their needs, this MEaSUREs project has the following goals**:

1. **Creation of a consistent long-term Earth System Data Record (ESDR) of the ocean surface vector winds** that includes observations from a number of different scatterometer missions while significantly improving the consistencies between them.
2. **Development of the dynamically-significant derived products** including the surface wind stress and the curl and divergence of the wind and the stress.
3. **Development of consistently formatted and user-friendly ESDR swath-based (Level 2) products (hereafter, L2)** featuring the above fields, including both scatterometer-based and model-based data collated with the underlying data.
4. **Development of scatterometer-only, consistently formatted and user-friendly gridded ESDR (Level 3) products** of the wind, stress, curl and divergence of the wind and the stress. These new ocean wind L3 products will fill an unmet user need and complement existing L4 products, which have their own roles.

1.1. Creation of a new ESDR of climate quality (or Climate Data Record – CDR)

The need of such efforts has been recognized by the IOVWST and the science community (Bourassa et al. 2009; Wentz et al., 2017). Indeed, more and more users employ scatterometer wind data for climate studies. However, the wind retrieval algorithms have been continuously improved over the years and the currently existing archives of near-real-time data are not always suitable to fulfill the need for homogeneous datasets spanning a longer period of time (Verhoef et al, 2017). When we say "homogeneous" we mean a dataset that is produced with consistent calibration, algorithms and assumptions, formatting (netCDF-4 with CF/ACDD/ISO-8601 compliance), quality flags/indicators, method of uncertainty quantification, and a consistent set of ancillary data.

There are two notable existing efforts that are in response to the need of creating extended ESDRs of climate quality:

i) the EUMETSATs OSI SAF scatterometer wind producer, the KNMI, is reprocessing several datasets to be published at a later time, with the QuikSCAT, ASCAT-A and ERS-1/2 CDRs being available now (https://scatterometer.knmi.nl/archived_prod/ and https://navigator.eumetsat.int/product/EO:EUM:DAT:METOP:OSI-150-B). The data are

compared to the NWP model and buoy winds. The stability of the wind characteristics is assessed and an attempt is made to attribute temporal changes to climatological and NWP model changes over time. (Verhoef et al, 2017).

ii) Addressing the needs for the creation of an *extended and homogeneous CDR* of the ocean surface winds, observed *by different instruments and missions*, the Remote Sensing Systems (RSS) devoted special attention to assuring the consistency of the retrievals that come from the different observing systems and over a prolonged period. The following have been processed as CDRs (cross-calibrated at all wind regimes): QuickSCAT (Ricciardulli and Wentz, 2015), ASCAT-A,-B,-C (Ricciardulli and Manaster 2021) - https://www.remss.com/announcement/ASCAT-ABC-ocean-surface-wind-CDR/).

However, scatterometer-based retrievals of ocean surface vector winds have uncertainties that come from several sources: the frequency and incident-angle-dependent GMF, the retrieval (inversion) algorithm and all its assumptions, and the frequency-dependent atmospheric corrections (especially concerning the corrections of the frequency-dependent rain contamination).

The effort described here provides an alternative set of retrieved products based on different retrieval algorithms (JPL's versus KNMI's versus RSS'), different GMFs, and the use of different nudge fields (NCEP versus ECMWF) that are needed to resolve the inherent ambiguity in the retrieved vectors. By developing the MEaSUREs-funded set of products we are now providing an additional ESDR of climate quality.

Only through analyses of a number of different ESDRs we can obtain a better understanding of the differences/uncertainties associated with the retrieval approaches and the creation of the ESDRs (Wentz et al., 2017). Such understanding is critically needed when analyzing the EDSRs to establish climate trends and variability, and to understand the processes and the evolution of the large-scale phenomena such as the MJO, ENSO and the Hadley Cell. Even the depiction of the diurnal variability of the winds might be affected by the different retrieval approaches.

1.2. New derived products

In addition to providing a new ESDR of the wind retrievals, this project develops a number of other products that are important for atmospheric, oceanographic, and climate studies: i) the surface wind stress; ii) spatial derivatives of the wind and of the stress.

- Surface wind stress: Based on the scatterometer ocean surface wind vectors, we develop and estimate of the ocean surface stress vector. Surface wind stress is a key variable of the earth system (e.g. GCOS-200) as it controls the circulation of the upper ocean. Today, surface wind stress fields are primarily estimated from wind products that blend wind observations from scatterometers, radiometers and model fields to develop space/time gap-free (interpolated) fields of the ocean surface winds, the so-called L4 products (e.g. the OAFlux products: https://climatedataguide.ucar.edu/climate-data/oaflux-objectively-analyzed-air-sea-fluxes-global-oceans). This introduces four sources of errors: i) errors that come from the blending of information from different sources, with different representativeness and error characteristics; ii) biases from missing observations in rain-flagged areas; iii) biases from estimating stress from averaged products; iv) aliasing from model output data functioning as a constraint, typically acting as a "smoother" which reduces outliers. These last two error sources are probably the most important due to the non-linear relationship between the wind

and the stress. Using the averaged winds to estimate the average stress will lead to underestimation of the stress. Instead, here we estimate the stress from the highest resolution, L2 wind products, thus preserving the accuracy of the stress estimates and properly reflecting their full dynamic range and spatial variability. In that, we follow similar approaches that have been adopted by EUMETSAT (OSI-SAF; produced by KNMI) – e.g. and https://resources.marine.copernicus.eu/product-detail/WIND_GLO_WIND_L3_NRT_OBSERVATIONS_012_002/INFORMATION – to produce estimates from a number of scatterometers, though in that case using somewhat different processing for the wind estimation from each one of the different instruments.

- Derivatives of the wind and of the stress: Spatial wind derivatives, such as vorticity and divergence, are important variables used to characterize low-level flow and derivatives of wind stress are fundamentally important for ocean forcing. Wind divergence is related to atmospheric convection and downdrafts within the atmospheric boundary layer (Kilpatrick and Xie, 2015). Wind vorticity characterizes the rotational movements of air and has been used to identify surface signatures of tropical disturbances, which can be precursors to tropical cyclones (Gierach et al. 2007). Wind stress curl is an especially important variable for characterizing large- and small-scale ocean forcing and for estimates of upwelling in the ocean. Wide-swath scatterometer winds are one of the only sources available for calculating spatial wind derivatives from satellites.

Wind/stress vectors and derivatives can also be found in the CMEMS (KNMI) daily scatt products (https://resources.marine.copernicus.eu/product-detail/WIND_GLO_WIND_L3_NRT_OBSERVATIONS_012_002/INFORMATION, incl. documentation; King et al., 2022). In that case, however, while both stress and derivatives are calculated at swath level (i.e., prior to the generation of any temporally-averaged product), they are calculated using regularly gridded (L3) wind field. Furthermore, they use wind vector estimates that have been produced somewhat differently from the observations from the different instruments/missions (e.g. at 25km resolutions for some versus at 12.5 km resolution for others.)

The goal of the project described here is to produce a long-term, *consistent record of stress estimates and the derivatives of wind and stress, using consistently-produced ocean surface wind vector retrievals from a number of different scatterometer instruments/missions* and computing the stress and the derivatives "in the swath" (i.e. without any spatial interpolation of the winds, an interpolation that is associated with gridding of the wind retrievals on a regular grid, prior the computation of the stress and the derivatives).

1.3. Developing Level 3 (L3) products (data coming soon)

Orbit-based L2 wind products (currently available at PO.DAAC) provide the most flexibility for use in fundamental scientific analyses by allowing each researcher to screen and aggregate the data based on the specific objectives of their studies. However, using these products requires each individual scientist to invest significant time and effort to build a robust understanding of the specifics of the measurements and the instrument capabilities and limitations. This expert knowledge is critical in determining the proper use of the data, as well as the flags. This can be remedied by the use of regularly gridded products with simplified flags. Such products come in two categories, Level 3 (L3) and Level 4 (L4), described in more detail below. The main difference between these two types of products is that the generation of L4 products requires the use of models and data

assimilation techniques to remove data gaps, thus introducing the model-specific characteristics in the final product. By contrast, L3 gridded products do not incorporate model data and thus are more consistent with the underlying L2 input data (they do not involve either space or time interpolation to fill the gaps between the orbital data). In addition, L3 products of the stress and the derivatives will come from gridding the L2 products of the same variables, avoiding sources of biases that come from computing stress and derivatives from interpolated in space/time L4 wind fields. Such L3 products will fill a niche while not competing with the existing Level 4 products that have their own roles.

The goal of this MEaSUREs project is to generate, for each scatterometer mission, three different L2 (Orbital) and three L3 (Gridded) products/files. Each L2 file contains one full orbital revolution starting at the southern-most latitude. The L2 products are targeted toward the specialists already accustomed to working with legacy L2 products. The L3 products will be simplified and targeted toward the needs of the larger user community. Each L3 file will contain the daily gridded products, separated into two fields – one for the ascending orbits and one for the descending ones.

Data products being developed under these efforts

Variable or other description	Spatial Extent & Resolution	Temporal Extent & Resolution	Remarks
Wind vector (EN and 10m): - Speed and direction - Zonal and meridional components (U and V) Stress vector: - Magnitude and direction - Zonal and meridional components Derivatives: - Curl and Divergence of the wind - Curl and Divergence of the stress	Resolution: - 12.5 km Spatial extent: - Swath	Temporal resolution: - Twice daily: ascending / descending Temporal Extent: - QuikSCAT – 1999-2009 - SeaWinds – 2003 - ASCAT-A – 2009 – present - ASCAT-B – 2014 - present - ASCAT-C – 2018 - present - RapidScat – 2014-2016 - ScatSat – 2017 – present	Level 2; Orbital data; Global coverage
Wind vector (EN and 10m): - Speed and direction - Zonal and meridional components (U and V) Stress vector: - Magnitude and direction - Zonal and meridional components Derivatives: - Curl and Divergence of the wind - Curl and Divergence of the stress	Resolution: 0.125 ^{0} Spatial extent: - Swath mapped on a grid		Level 3; Gridded; Global Coverage

2. Product Files – Overview of product types, content, location and formats

2.1. Types of files

The new products are organized in **three types** of files that will be available for both the L2 and the L3 files, and based on observations from QuikSCAT, ASCAT-A/B/C and ScatSat:

- **Scatterometer-based estimates** of the Equivalent Neutral (EN) wind, the stress and the 10m true wind (accounting for the stability of the atmosphere, and for the surface currents). For each of these fields, the files include: the magnitude and the direction; the zonal and meridional components; the uncertainty in magnitude and direction; a number of traditionally-used quality flags; a new, and simplified, Quality Indicator flag (values 0-5), in addition to the number of quality flags used in the past, to help the users more easily navigate the maze of flags.
- **Ancillary data** - collocated in space and time wind/stress data from ERA-5 (including SST, surface pressure, 2m temperature and relative humidity), surface precipitation from IMERG, and the surface currents from GlobeCurrents. The goal of these ancillary data is to support the evaluation of the new products
- **Derivatives of the wind and the stress** (will be produced soon). These files will contain the following derivative fields: Curl and divergence of the EN wind; Curl and divergence of the stress; Curl and divergence of the 10m real wind; Same from ECMWF-ERA5 fields.

2.2. Data location for the current release of L2 products

The Version 1.0 data are in NetCDF-4 format and are available from PO.DAAC:
https://podaac.jpl.nasa.gov/datasetlist?values=MEaSUREs/OSWV&view=list&ids=Projects

- ASCAT-A L2 Wind and Stress Vectors – DOI: https://doi.org/10.5067/ESASA-L2W10
- ASCAT-A L2 Modeled Auxiliary Fields – DOI: https://doi.org/10.5067/ESDAA-L2C10
- ASCAT-B L2 Wind and Stress Vectors – DOI: https://doi.org/10.5067/ESASB-L2W10
- ASCAT-B L2 Modeled Auxiliary Fields – DOI: https://doi.org/10.5067/ESDAB-L2C10
- QuikSCAT L2 Wind and Stress Vectors – DOI: https://doi.org/10.5067/ESDQS-L2W10
- QuikSCAT L2 Modeled and Auxiliary Fields - DOI: https://doi.org/10.5067/ESDQS-L2C10
- SCATSAT-1 Wind and Stress Vectors – DOI: https://doi.org/10.5067/ESDSS-L2W10

2.3. File Formats

The data files are provided in netCDF-4 format using internal compression and adhering to the following metadata standards: ISO-8601, ACDD version 1.3, and CF version 1.8.
The complete listing of science data variables and associated metadata can be found by executing the following command using your terminal/console:

ncdump -h <filename>.nc

The "ncdump" utility is open-source and is installed by default as part of the netCDF-4 package, which can be obtained here: https://www.unidata.ucar.edu/software/netcdf/. More information on the "ncdump" utility can be found here:
https://www.unidata.ucar.edu/software/netcdf/documentation/NUG/netcdf_utilities_guide.html#ncdump_guide

A "quick" view (2-D mapped plotting) of the netCDF data and metadata can also be performed through the free and open-source Panoply data viewer application, which can be installed on Windows, Mac OSX, and Linux. The latest version of Panoply can be obtained here:
https://www.giss.nasa.gov/tools/panoply/

README files that will serve as a quick reference guide to the MEaSUREs ESDR products, can be found within each of the dataset landing pages listed by DOI in the previous section.

3. L2 (Orbital/Swath) data files.

Each data file corresponds to a specific orbital revolution number, in which the starting point of the file is defined by the beginning of the ascending node of the orbit at the southernmost latitude of the orbit; the ending point of the file is defined by the end of the descending node of the orbit. The following coordinate variables are provided to establish geospatial and temporal placement of data sampled within the swath: time (UTC, expressed in units of seconds since 1999-0101-01 00:00:00), lat (latitude, expressed in units of degrees), and lon (East longitude, expressed in units of degrees in absolute coordinates ranging from 0 to 360). Wind data elements are given as both vector magnitude and direction (from North) and as zonal and meridional (East, North) components.

3.1. The L2 scatterometer data products

3.1.1. File content

- Time – time data and units should be referenced to "seconds since 1999-01-01 00:00:00.0"
  - follows legacy QuikSCAT time variable convention.
- Lat/Lon
- a comprehensive set of flags (updated from QuikSCAT herritage)
  - flags
  - _FillValue = -1
  - valid_min = 0
  - valid_max = 526352355
  - long_name = quality flags
  - units = bit
  - coordinates = lon lat
  - flag_masks = 1, 2, 32, 64, 128, 256, 512, 1024, 2048, 4096, 8192, 16384, 65536, 131072, 262144, 524288, 1048576, 4194304, 16777216, 33554432, 67108864, 134217728, 268435456
  - flag_meanings = adequate_sigma0_flag adequate_azimuth_diversity_flag poor_coastal_processing_flag wind_retrieval_likely_corrupted_flag coastal_flag ice_edge_flag winds_not_retrieved_flag high_wind_speed_flag low_wind_speed_flag rain_impact_flag_not_usable_flag rain_impact_flag missing_look_flag rain_correction_not_applied_flag correction_produced_negative_spd_flag all_ambiguities_contribute_to_nudging_flag large_rain_correction_flag coastal_processing_applied_flag lake_winds_flag rain_nearby_flag ice_nearby_flag significant_rain_correction_flag rain_correction_applied_flag wind_retrieval_possibly_corrupted_flag
- a simplified quality indicator flag (new)
  - quality_indicator
  - _FillValue = -1s
  - valid_min = 0s

- valid_max = 5s
- long_name = simplified quality classification based on applied flags
- units = -1
- coordinates = lon lat
- flag_masks = 0s, 1s, 2s, 3s, 4s, 5s
- flag_meanings = no retrieval corruption, insignificantly corrupted retrieval, possible significant error, likely significant error, no winds retrieved due to quality control, no data over liquid water in cell

- Equivalent Neutral wind speed and direction, EN wind zonal and meridional components
- Wind stress magnitude and direction, wind stress zonal and meridional components.
- 10m true wind magnitude and direction, zonal and meridional components. The wind speed and vector components represent true wind speeds 10 m above the ocean surface assuming that a log-layer is valid to this height. This definition DOES NOT assume a neutral boundary-layer stability. The true wind estimates have also accounted for the ocean currents (i.e., they are no any longer surface-relative.
- Uncertainty - the most necessary information on the uncertainty of magnitude, direction and components of the: EN wind; stress; 10m true wind.

3.1.2. File naming convention:

- **QuikSCAT :**
  measures_esdr_qs_l2_wind_stress_RRRRR_vN.n_sYYYYMMDD-HHMMSS-eYYYYMMDD-HHMMSS.nc
  - measures NASA Program identifier.
  - esdr MEaSUREs product identifier; esdr = Earth System Data Record.
  - qs Platform/Instrument identifier: qs = QuikSCAT.
  - l2 Processing Level identifier: l2 = Level 2.
  - wind_stress Primary science data variables contained within this product.
  - RRRRR 5-digit orbital revolution number.
  - VN.n Version ID, where N = primary version; n = incremental release number.
  - s Start date and time separator of the first data in the file in UTC.
  - e End date and time separator of the last data in the file in UTC.
  - YYYY 4-digit year in UTC.
  - MM 2-digit month in UTC.
  - DD 2-digit day of month in UTC.
  - HH 2-digit hour of 24-hour in UTC.
  - mm 2-digit minute of hour in UTC.
  - .nc File extension: nc = netCDF

- **ASCAT-A :**
  measures_esdr_metopa_as_l2_wind_stress_RRRRR_v1.0_sYYYYMMDD-HHMMSS-eYYYYMMDD-HHMMSS.nc
  - same as for QuikSCAT above except for
  - as_metopa Platform/Instrument Identifier: as = ASCAT; metopa = MetOp-A platform.
- **ASCAT-B :**

- measures_esdr_metopb_as_l2_wind_stress_RRRRR_v1.0_sYYYYMMDD-HHMMSS-eYYYYMMDD-HHMMSS.nc
  - same as for ASCAT-A above except for
  - metopb = MetOp-B platform.
- **SCATSAT-1 :**

measures_esdr_scatsat_as__l2_ancillary_RRRRR_vN.N_sYYYYMMDD-HHMMSS-eYYYYMMDD-HHMMSS.nc

  - **same as for QuikSCAT above except for**
  - scatsat Platform/Instrument Identifier

3.1.3. Data sources

- QuikSCAT
  - the scatterometer EN wind retrievals are copied from the L2B v4.1 QuikSCAT retrievals; DOI: 10.5067/QSX12-L2B41. These winds were produced using the KuSST GMF (Ricciardulli and Wentz, 2017) that was developed as an additive adjustment to be applied to the Ku-2011 GMF (Ricciardulli and Wentz (2015). KuSST was developed to remove the diagnosed from observations SST-dependence of the Ku-band scatterometer σ_o, that was established by binning the σ_o in Reynolds SST bins. As such, the SST-dependent modifications of the GMF were not developed with the use of other wind retrievals.
  - the stress estimates and the 10m true winds are based on the EN winds. Stress is estimated from the EN winds as described further in Section 4. The 10m true winds are estimated again from the EN QuikSCAT winds, with the help of data describing the atmospheric state as depicted by the hourly ERA-5 analyses, interpolated in time to the scatterometer observations.
- ASCAT-A/B
  - the scatterometer retrievals of the EN winds were produced: using the JPL **retrieval algorithms and ancillary data** – the NCEP model fields were used for nudging. Note, as described later, the ERA-5 *forecast fields* are used for evaluation to avoid incestuous use of
    - the same scatterometer data in *the analyses* and then *for validation*
    - the same model data for nudging and then for evaluation (NCEP vs ERA-5)
  - the JPL ASCAT retrievals are based on:
    - the ASCAT L1B measurements. Our project could not have gone forward without the great support we received from Stefanie Linow (Stefanie.Linow@eumetsat.int) and Debbie Richards, both from EUMETSAT. We really appreciate their critical help in providing us with the L1B SZF data in the native format (not HDF), containing the full resolution sigma0 observations. These were the CDR for ASCAT-A and GDS for ASCAT-B
    - the use of a new GMF – $CMOD7_{JPL}$, based on CMOD7. Its development is described in Section 4.
  - the stress estimates and the 10m true winds are based on the EN winds, similarly to the QuikSCAT retrievals

3.2. The L2 ancillary data products

3.2.1. Overview and purpose

One ancillary file is produced for every L2 scatterometer data file. These products represent an overlay – they are provided on the same grid as the main scatterometer data file and are also interpolated in time to the scatterometer observation time. The intended purpose of the ancillary data is to provide inputs for evaluation of the scatterometer products.

3.2.2. File content:

- **ERA-5 Forecast Model Wind Data (for more information, see section 3.2.4 on the matching of the ERA-5 short-term forecasts and the scatterometer winds):**
  - EN 10m wind, wind stress, and the 10m true wind, given as magnitude, direction and components.
- **ERA-5 Model Analysis Data (used in production of L2 real wind products):**
  - Sea surface temperature
  - 2m air temperature
  - Boundary layer height
- **GPM IMERG**
  - GPM IMERG Precipitation Rate
- **Globcurrent:**
  - Components of vector total currents and stokes drift.
- **Duplicated fields from the L2 scatterometer data products**
  - Flags
  - Quality indicator

3.2.3. File naming convention:

- **QuikSCAT: measures_esdr_qs_l2_wind_stress_RRRRR_vN.n_sYYYYMMDD-HHMMSS-eYYYYMMDD-HHMMSS_ancillary.nc**
  - measures NASA Program identifier.
  - esdr MEaSUREs product identifier; esdr = Earth System Data Record.
  - qs Platform/Instrument identifier: qs = QuikSCAT
  - l2 Processing Level identifier: l2 = Level 2.
  - wind_stress Primary science data variables contained within the Scatterometer product.
  - RRRRR 5-digit orbital revolution number.
  - VN.n Version ID, where N = primary version; n = incremental release number.
  - s Start date and time separator of the first data in the file in UTC.
  - e End date and time separator of the last data in the file in UTC.
  - YYYY 4-digit year in UTC.
  - MM 2-digit month in UTC.
  - DD 2-digit day of month in UTC.
  - HH 2-digit hour of 24-hour in UTC.
  - mm 2-digit minute of hour in UTC.
  - ancillary MEaSUREs ESDR Ancillary product type identifier.
  - .nc File extension: nc = netCDF

- **ASCAT-A: measures_esdr_metopa_as__l2_ancillary_RRRRR_vN.N_sYYYYMMDD-HHMMSS-eYYYYMMDD-HHMMSS.nc**
  - **same as for QuikSCAT above except for**
  - as_metopa Platform/Instrument Identifier: as = ASCAT; metopa = MetOp-A platform.
- **ASCAT-B: measures_esdr_metopb_as__l2_ancillary_RRRRR_vN.N_sYYYYMMDD-HHMMSS-eYYYYMMDD-HHMMSS.nc**
  - **same as for ASCAT above except for**
  - metopb = MetOp-B platform.
- **SCATSAT-1: measures_esdr_scatsat_as__l2_ancillary_RRRRR_vN.N_sYYYYMMDD-HHMMSS-eYYYYMMDD-HHMMSS.nc**
  - **same as for QuikSCAT above except for**
  - scatsat Platform/Instrument Identifier

3.2.4. Data Sources

All data sources were interpolated in space and time using linear interpolation to the scatterometer swath. [This is repeated in each item below, but probably OK for clarity/specificity.] Specifics for each data source are given below:

ECMWF ERA5 Forecast Fields: ERA5 ***forecast fields*** were chosen for wind-related variables such that comparisons can be made between scatterometer winds and the ERA5 forecasts without worry of scatterometer fields being assimilated into the comparison model. ERA5 forecasts are run twice daily at 30km resolution, initialized from the 06Z and 18Z analysis fields. To reduce the impact of the analysis initialization, the forecast hours we used are hours 4-16, corresponding to hours 10Z-21Z for the 06Z forecast cycle, and hours 22Z-09Z for the 18Z forecast cycle. These hourly observations were interpolated to the scatterometer swath using linear interpolation in space and time. These data were accessed from the ECMWF MARS catalog: https://apps.ecmwf.int/data-catalogues/era5/?class=ea

ECMWF ERA5 Analysis Fields: ERA5 reanalysis fields were chosen for all other variables of interest. ERA5 reanalysis is run hourly at 30km resolution, which is the source sampling used for these fields. These hourly fields were interpolated in space and time to the scatterometer swath. These data were accessed from the ECMWF MARS catalog: https://apps.ecmwf.int/data-catalogues/era5/?class=ea

Globcurrent Surface Currents: The Globcurrent project (http://globcurrent.ifremer.fr/) produces estimates of ocean surface currents representing various physical processes (e.g. Rio et al., 2014). We selected two of these to include in this ancillary data product: the total surface current and the stokes drift. The total surface current, in the case of Globcurrent, represents the sum of geostrophic currents estimated using altimetry and Ekman currents estimated using a wind parameterization (Rio et al., 2014). Stokes drift, estimated using WaveWatch III, is provided separately. Detailed information on these two products is available at globcurrent.org. Primarily missing from these estimates of surface currents are the tidal, inertial, and internal wave components.

The Globcurrent source total surface current field is estimated at .25 degree resolution every three hours. The Stokes drift is estimated at .5 degree resolution every 3 hours. Especially in the case of the geostrophic component in the total surface current product, the true spectral resolution

is likely on the order of 100-200km and 1-2 weeks. Both the total surface current fields and the stokes drift are linearly interpolated in space and time to the scatterometer swath from the Globcurrent V3 dataset available at http://tds0.ifremer.fr/thredds/GLOBCURRENT/GLOBCURRENT.html .

GPM IMERG Precipitation Rate: The Integrated Multi-satellitE Retrievals for GPM (IMERG - https://gpm.nasa.gov/) estimates precipitation relevant parameters using an intercalibrated set of radiometers and radar instruments (e.g. GPM IMERG ATBD). Multiple resolutions and data fidelities are available from IMERG. This project selected the .1 degree, half hourly, final calibrated V6 data product available here: https://disc.gsfc.nasa.gov/datasets/GPM_3IMERGHH_06/summary. Only the calibrated precipitation rate is interpolated in time and space to the scatterometer swath.

4. What is in new in the data and how the new products were developed

4.1. ASCAT-A/B

The main goal of our project is to produce scatterometer wind and stress estimates that are consistent when taking as input observations from different instruments, that use different frequencies, incidence angles and observing geometry.

As mentioned in the introduction, the scatterometer-based retrievals of ocean surface winds have differences/uncertainties that come from several sources: the frequency- and incident-angle-dependent GMF, the retrieval (inversion) algorithm and all its assumptions, and the frequency-dependent atmospheric corrections.

To avoid these sources of inconsistency in the climate data record we are developing, we take the following approach: i) develop a GMF for C-band using the Ku-wind retrievals as truth; ii) utilize consistent measurement resolution by retrieving winds on the same resolution grid with the same measurement binning method; iii) convert (NRCS) σ^0 measurement to winds using the same (JPL's) wind retrieval algorithm and the same ancillary data (e.g., NCEP model fields) for nudging.

Below is a quick description of the efforts to harmonize the retrievals made from QuikSCAT observations and those made from ASCAT-A (i.e., the development of the new C-band GMF). We began by producing wind retrievals from 3 years of ASCAT-A observations, using the KNMI CMOD7 GMF (Stoffelen et al, 2017) and the JPL retrieval algorithms and ancillary data. A comparison to the retrievals from collocated in space and time (to within 90 min time differences, and within rain-free regions) QuikSCAT observations showed that some differences remained, prompting the need for the development of a modified GMF.

We then fit a polynomial mapping between the Ku- band (JPL algorithm and using KuSST GMF) and C-band (JPL algorithm, CMOD7 GMF) retrieved wind speeds. The polynomial mapping between Ku and C retrieved wind speeds serves as the basis for the development of a modified C-band GMF. We call that $CMOD7_{JPL}$ (or $CMOD7_{adjusted}$) as it was developed starting with CMOD7 (KNMI) and modifying it to achieve winds that are "homogeneous/harmonized" with QuikSCAT retrievals.

Figures 1 and 2 illustrate how the ASCAT-A and QuikSCAT retrievals, from collocated measurements, compared originally and after the adoption of the adjusted GMF.

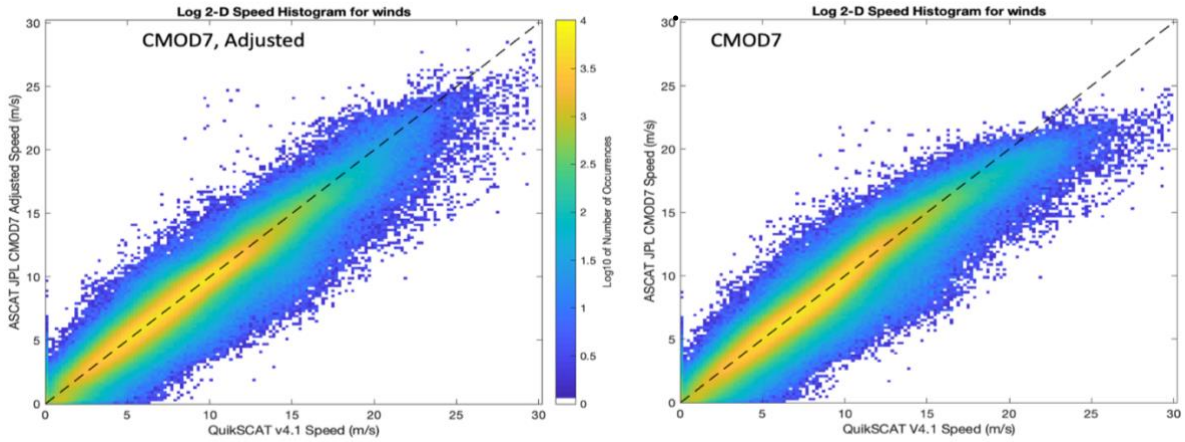

Figure 1: Two dimensional joint histograms of ASCAT and QuikSCAT retrieved wind speeds. The Y-axis is ASCAT speed. The X-axis is QuikSCAT speed. If the two instruments produced identical winds they would cluster along the black dashed one-to-one line. The left panel shows the ASCAT retrieval with the QuikSCAT-adjusted CMOD7 GMF. The right panel show ASCAT retrieval using the original CMOD7 GMF. As it was constructed to do, the adjusted GMF results in better agreement between the two sensors. The primary improvement is an increase in ASCAT winds over 15 m/s to match QuikSCAT. There is also a reduction in the slight meandering of the distribution along the one-to-one line for lower winds.

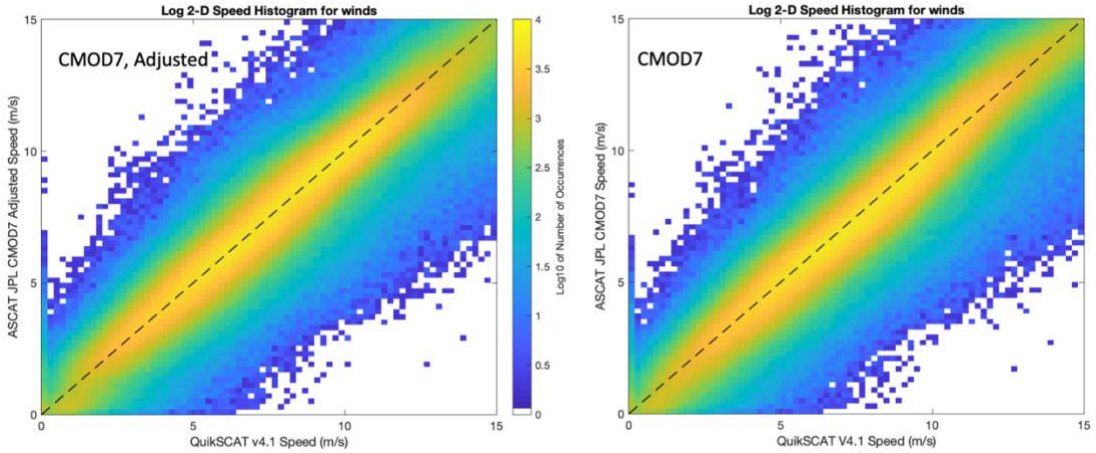

Figure 2: Panels from Figure 1 are expanded to better illustrate the difference in the retrieved speeds from the two GMFs for 0 to 15 m/s winds.

Figure 3 illustrates the impact the new GMF has on the Probability Density Function (PDF) of the retrieved winds. Provided here is the comparison in the PDF distributions for four types of retrievals, from the same collocated observations. It also illustrates the variation in the PDF for different SST regimes. Ku-band scatterometers are more sensitive to SST-induced effects than C-band scatterometers (Wang, Stoffelen et al, 2017; Ricciardulli Manaster 2021). Although, the QuikSCAT wind retrieval makes use of external SST data to minimize wind speed effects due to SST, the procedure is imperfect and so there is likely a small residual error due to SST in QuikSCAT wind speeds. As shown in Figures 1 and 3, the adjusted C-band GMF greatly reduces the disagreement between ASCAT and QuikSCAT at high winds but it doesn't entirely remove it. This may be due to saturation of sigma-0 and thus reduced sensitivity in VV polarized C-band measurements at high wind speeds.

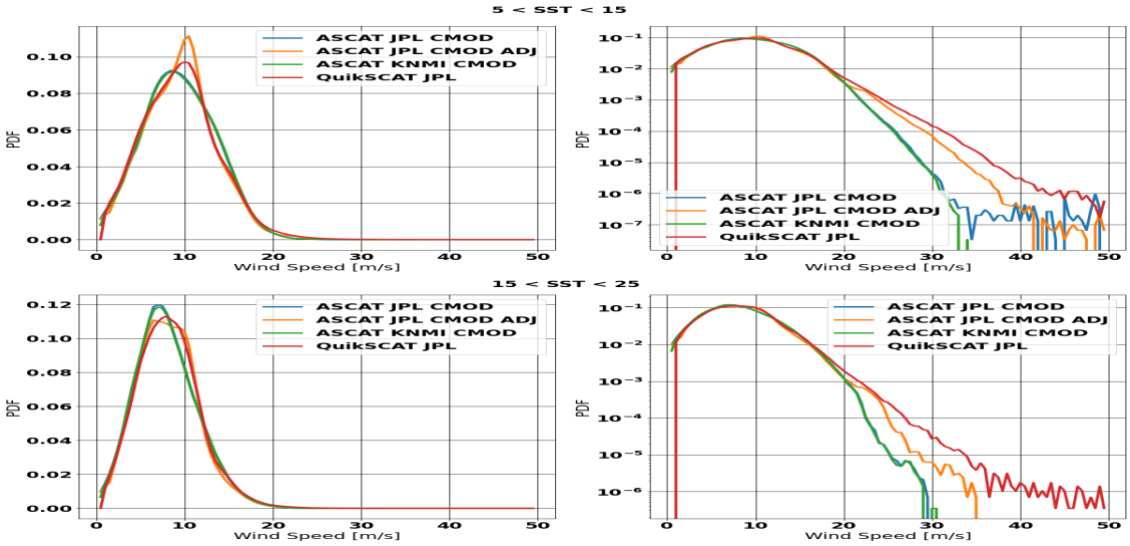

Figure 3. Univariate (single parameter) Probability Density Functions (PDFs) for four types of retrievals from collocated observations, shown in four different colors in each of the four panels – $ASCAT_{KNMI\text{-}CMOD7}$ in green; $ASCAT_{JPL\text{-}CMOD7}$ in blue, $ASCAT_{JPL\text{-}CMOD7ADJ}$ (or $ASCAT_{JPL\text{-}CMOD7jpl}$) in orange; $QuikSCAT_{JPL\text{-}KuSST}$ in red. The top and bottom panels show comparisons for two different SST regimes (5<SST<15 deg C in the top panels; 15<SST<25 deg SST in the bottom panels). Left column shows comparisons of the PDFs on the linear scale, revealing the PDF differences in the dominant wind regimes. The right column shows the PDF comparisons on the log scale, revealing the PDF differences in the tales of the distributions.

4.2. New QuikSCAT/ASCAT products

There are several new products that will be included in all scatterometer products to be released as part of the MEaSUREs project, including the QuikSCAT retrievals that are now based on the V4.1 version released in the past.

4.2.1. Stress

Surface wind stress is a key variable of the earth system (e.g. GCOS-200) as it controls the circulation of the upper ocean. Surface wind stress fields are often estimated from gridded L4 wind products that blend wind observations from scatterometers, radiometers and model fields to develop space/time gap-free (interpolated) fields of the ocean surface winds. This type of L4 stress product can contain at least four important error sources: i) errors that come from the blending of information from different sources, with different representativeness and error characteristics; ii) biases from missing observations in rain-flagged areas; iii) biases from estimating stress from averaged products; iv) aliasing from model output data functioning as a constraint, typically acting as a "smoother" which reduces outliers. The latter two are probably most important due to the non-linear relationship between wind and stress. For example, using averaged winds to estimate the average stress leads to stress underestimation.

Similar to efforts at EUMETSAT (OSI-SAF; produced by KNMI) – e.g. https://navigator.eumetsat.int/product/EO:EUM:DAT:METOP:OSI-150-B - this project provides L2 scatterometer wind stress estimates derived from the highest resolution, swath-based wind products, however the difference is that here we estimated the stress on the L2 swath, prior any interpolation related to re-gridding on a regular lat/lon grid (i.e. from the L2 products and not from the L3

products). This preserves vector wind stress estimate accuracy and properly reflects the full dynamic range and spatial variability that can be obtained using the scatterometer.

The key factor needed to derive wind stress data from scatterometer 10m EN winds is the drag coefficient (C_d), a term parameterizing the effective surface aerodynamic roughness. The recent paper of de Kloe et al. (2017) provides a review of the issues surrounding validation and potential biases involved in the supposed equivalence between the true observed wind stress (τ), friction velocity (u_*), and the satellite scatterometer 10m equivalent neutral wind data (U_{10EN}) relative to the ocean surface provided by the data centers where the vector stress is given by

$$\boldsymbol{\tau} = \rho_a \cdot |\mathbf{u}_*| \, u_* = \rho_a \cdot C_{D10EN} \cdot |\mathbf{U_{10EN}}| \, U_{r10EN} \qquad (1)$$

where ρ_a is the air density and C_{D10EN} the neutral drag coefficient (C_d hereafter).

An implicit advantage to having equivalent-neutral stability wind observations is that this drag coefficient does not have to be adjusted for varying boundary layer stability conditions.

Numerous C_d models exist, with many scatterometer wind stress applications using the Large et al. (1994) formulation. But more recent and improved *in situ* wind stress data and experiments indicate that latest C_d algorithms (Kudryavtsev and Makin, 2001; Bourassa, 2006; Drennan et al. 2005; Suzuki et al. 2013; Edson et al., 2013) differ considerably from Large et al. (1994) formulation, especially at wind speeds above 10 m/s. Edson et al. (2013) produced a wind-dependent drag formulation over the open-ocean that shows good agreement with both field observations and global reanalysis datasets. This $C_d(U_{10EN})$ model is contained in the Coupled Ocean-Atmosphere Response Experiment (COARE) version 3.5 algorithm (Edson et al., 2013). Our project evaluated several of the more commonly used drag coefficient models including assessment of their consistency with recent field studies and impact on wind stress product uncertainty using satellite and in situ air-sea flux data matchups as shown in Fig. 4. Candidate buoy C_d models included Large et al. (1994), Liu and Tang (1996), COARE3.5, and a linear model from deKloe et al. (2017) that is employed for ASCAT wind stress data products produced by KNMI (noted as KNMI in Figs. 4 and 5). The assessments that can be made with the limited buoy stress data in hand (Fig. 4) indicate that the Large et al. model would lead to stress underestimation at winds above about 8 m/s and that the linear wind-

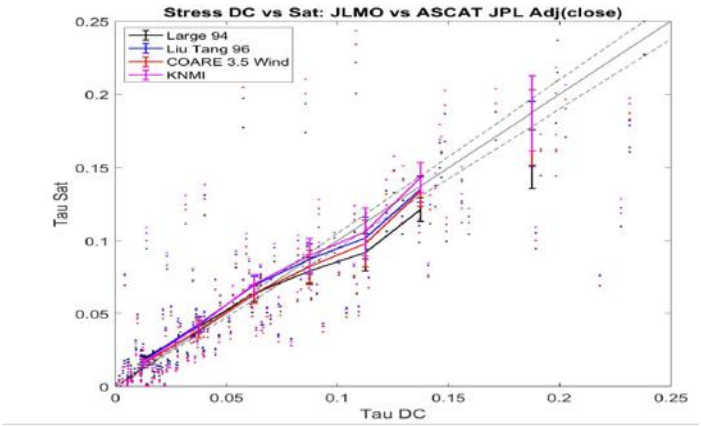

Figure 4. Comparison of stress estimates made from satellite observations to buoy eddy covariance flux observations. The comparisons are done using four different bulk formulas for the drag coefficient as noted in the text.

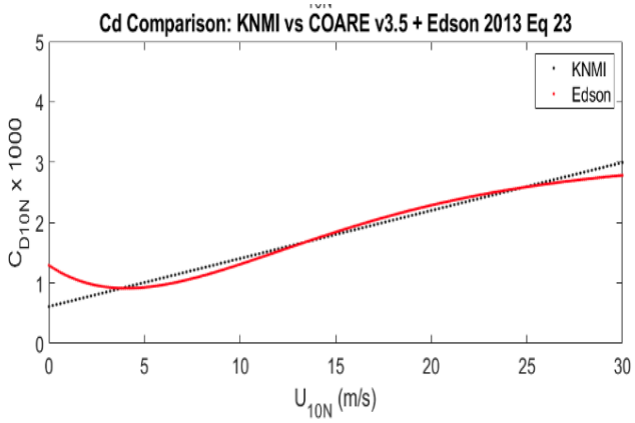

Figure 5. The drag coefficient model used in the V1.0 release of the MEaSUREs product

dependent KNMI model agreed well enough with COARE3.5 as to be equivalent for wind speeds up to 20 m/s (see Fig. 5). Given that this C_d model is already in use for ASCAT data production (Copernicus Marine Environment Monitoring Service, CMEMS L3), is simple to implement as a first-cut MEaSUREs version, and can be improved in future versions, we chose to adopt this following KNMI C_d model for the L2 stress estimates in these stress data products. **The model is C_d = a*(U10EN) + b,**

where a=7.94e-5 and b = 6.12e-4.

This version-1 wind stress drag coefficient algorithm performed well in first direct comparisons of both ASCAT and QSCAT L2 stress against in situ buoy stress derived from 20 min. direct covariance flux estimates as seen in Figs. 4 and 6, across winds from 3-15 m/s. The data come from buoy-satellite matchups of direct covariance flux measurements collected in the Gulf of Maine on the UNH Jeffreys Ledge Moored Observatory (JLMO) platform from 2007-2009.

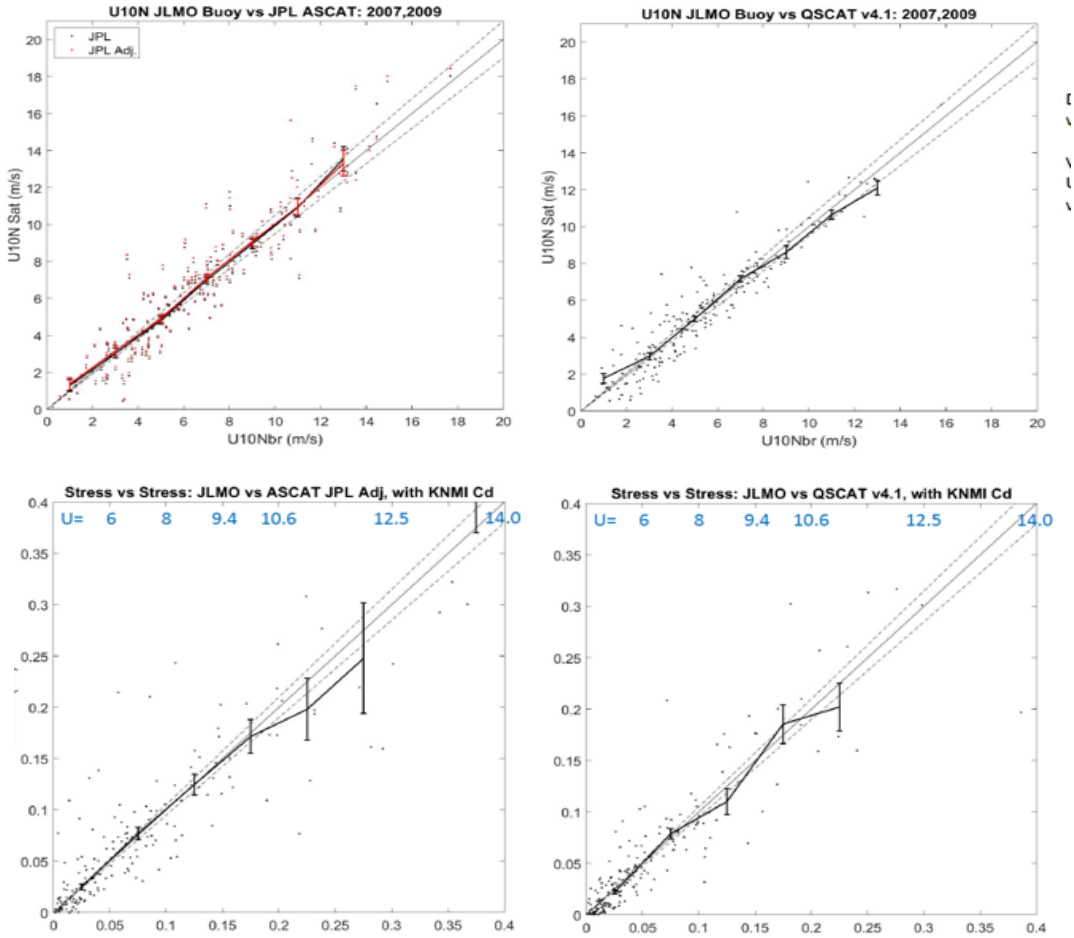

Figure 6. Wind (top panels) and stress (bottom panels) matchups at flux buoy deployments show no obvious systematic biases but the available data are limited. A more extensive set of buoy measurements will be employed as the MEaSUREs dataset expands.

Any future modification of the form for the L2 stress product drag coefficient can be addressed and validated only if there is access to a much larger flux buoy dataset. Towards that end, we continue to process and improve raw buoy eddy covariance flux observations from the open ocean NSF OOI air-sea flux buoys in the Southern Ocean, Irminger Sea, NE US shelf and Oregon shelf for

collocation against ScatSat and ASCAT-A and -B data in the 2014-2020 time period. This will significantly expand wind stress verification efforts. This is an important step, done in preparation for the next phase of the project when ScatSat calibration will be performed and ScatSat/ASCAT comparisons will be analyzed – both in terms of retrievals of stress-equivalent neutral 10 m winds, and in terms of the derived surface stress.

4.2.2. True 10m Winds

Scatterometers are sensitive to the roughness of the ocean's surface. Through GMFs, we convert scatterometer measurements of roughness into "winds." However, this surface roughness is not generated by the wind per-se, but instead by the wind stress. As discussed above, the wind stress (τ) is related to the wind speed by $\tau = \rho_a * Cd * (U_{10}-U_S)|U_{10}-U_S|$. Note the difference between U_{10} and U_S; this is referred to as the moving reference frame, or the "relative winds" [U_S = surface-relative speed, i.e., including currents]. In terms of scatterometer data products this stress is written as $\tau = \rho_a * C_{D10EN} * U_{10EN} * |U_{10EN}|$.

By training scatterometer GMFs to transform between winds and surface roughness, we are really training to go between stress equivalent winds given a neutral boundary layer and surface roughness. The question we like to address is: Can we make an adjustment to our resulting stress equivalent neutral winds to give something that more closely resembles "true winds?"

Estimating the "true" winds is an important step towards reconciling in-situ wind measurements with remotely sensed scatterometer wind data, which can exhibit persistent differences in regions of strong currents or SST fronts.

We developed a system to estimate the "true" 10-meter winds from scatterometer data. This set of software pulls in ancillary sea surface temperature, planetary boundary layer height, and air temperature from ECMWF ERA-5 analyses, along with surface current from the GlobCurrent project, and combines them with scatterometer stress-equivalent 10-meter neutral winds (EN winds) to estimate the "true" 10-meter winds.

The COARE 3.5 algorithm was implemented in Python to perform atmospheric stability corrections and surface stress/mixing estimates. The COARE 3.5 algorithm iteratively solves the equations of momentum, temperature, and humidity stratification in the boundary layer (Liu et al. 1996). Typically, this algorithm is used to solve for a wind speed under neutral conditions, given wind speeds under non-neutral conditions. We modified COARE to do the opposite: take input EN winds from scatterometers, in addition to ancillary data, to produce an estimate of the true 10 meter *surface-relative* wind.

COARE can take many input parameters, some of which were left as constants, while others were taken from 30km ERA5 hourly analysis fields interpolated to the scatterometer swath.

- From ERA5:
  - Air temperature (2 m)
  - Surface air pressure
  - Sea surface temperature
  - Boundary layer height
  - Relative humidity computed using Magnus approximation
- From scatterometer retrievals:
  - Equivalent neutral wind speed (relative neutral wind)

With the 10 meter *surface-relative* (non-neutral) wind estimated with COARE, vector surface currents from the GlobCurrent project were added in simple summation to produce the estimated true (*absolute, not surface relative anymore*) 10-meter wind vectors.

- From GlobCurrent:
  - Total surface currents, equal to geostrophic plus Ekman
  - Stokes drift

All GlobCurrent data was taken from the V3 product at 3 hourly resolution. The Stokes drift is estimated at 0.5 degree resolution while the total currents are estimated at .25 degree resolution. Since this is a vector sum, the addition of surface currents will result in a changed wind speed and direction.

Due to the many data sources involved in producing the real winds product, data files may be missing when source input data was not available. This missing data occurs sporadically in time and always in some inland lakes/seas, notably the Mediterranean Sea.

Figure 7 illustrates the difference between the EN winds and the 10m true winds for one month of data. In regions with strong surface currents, like the Southern Ocean, for example, the persistent Eastward blowing wind and Eastward currents significantly reduce the surface stress compared to the real wind. This results in a strong positive correction in the real wind product. The other place where this correction is substantial is in areas of large sea-air-temperature difference, for example off the coast of Alaska here. Owing to the bulk calibration done in scatterometer data, and to the GMF training, the average correction globally is likely very close to zero. But most areas around the globe have substantial ~1 m/s scale adjustments between real wind and EN wind. Comparisons between scatterometers and in-situ real wind data would be wise to take this into account, especially if regional influence from currents or SST is expected.

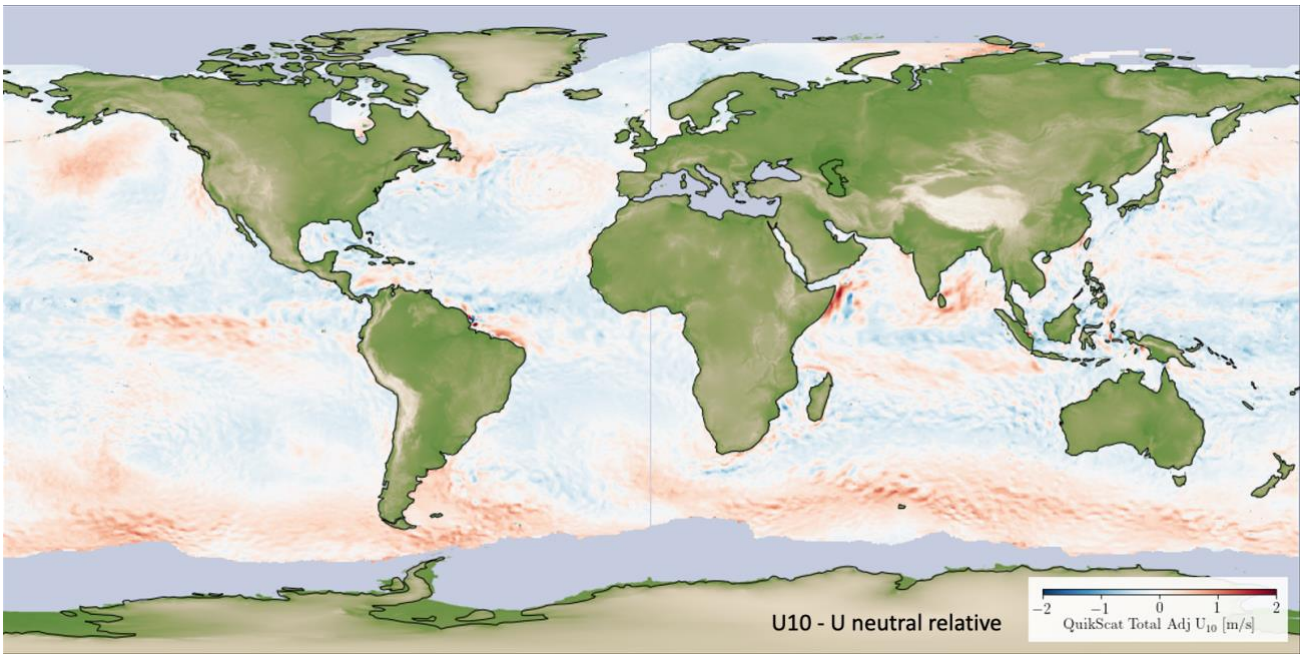

Figure 7. Map of the differences between the 10m "true" winds and the "~~Stress~~ Equivalent Neutral (EN)" winds.

The performance of the 10m true winds product was evaluated against ECMWF 10-meter wind data and against buoy in-situ wind data, using a limited set of data. Each of these datasets showed a slightly improved correlation to the new true wind products than to the scatterometer ~~stress~~

equivalent neutral winds. As Fig. 7 illustrates, the difference between true 10m winds versus the EN winds has stronger regional significance than bulk statistics might imply.

4.2.3. Quality Indicator

Traditionally, scatterometer surface wind retrieval products include a significant number of flags that indicate the quality of each individual retrieved value. These flags are meant to attest to: the quality of the input data, the proximity of land or ice that could be contaminating the original measurements, the presence of rain within the scatterometer field of view, or other assumptions and factors that might adversely affect the quality of the retrievals.

Our new products continue the tradition and provide a number of flags used in the past. These flags are there to help the experienced researcher to weed out retrievals with questionable value, according to their specific research interests. However, the rules to use these flags might also be very cumbersome. In reality, their use could also create confusion among the new users with less familiarity with scatterometer data and retrieval approaches.

Here, for the first time, we also provide a more general Quality Indicator (QI), to help the users more easily navigate the maze of flags. The quality indicator in the Level 2 (orbital) data files developed by our MEaSUREs project is an integer between 0 and 5 that denotes *the quality category* of the data, with 0 being the highest quality and 5 the lowest.

Here the general description:

Category 0: No retrieval corruption
Category 1: Insignificantly corrupted retrieval
Category 2: Possible Significant Error
Category 3: Likely Significant Error
Category 4: No winds retrieved due to quality control
Category 5: No data over liquid water in cell (i.e., land, ice, etc. data)

We have performed extensive evaluation on whether the Quality Indicator:

- Has been properly designed – in response to our intentions as described by the 5 categories above.
- Has been set correctly according to our rules

More detailed information on the meaning of Quality Indicator categories is provided below.

Here is a quick description of the data included in each of the five categories, and recommendation to the users of the Quality Indicator.

4.2.3.1.QuikSCAT

- **Quality Indicator 0** – No Retrieval corruption - the best possible retrievals; to be used when needing highest quality data – e.g. for development of GMFs
  - data that is not flagged as rainy and no rain correction was applied in the cell, or in any cell within surrounding 7 by 7 neighborhood on the 12.5-km grid. It excludes data with ice in the 7 by 7 neighborhood, or with poor coastal retrievals or negative wind speeds. *It includes only dual beam (HH and VV) data*

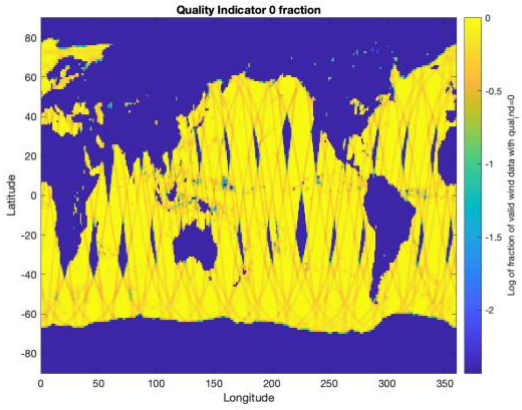

- The data set comprises 73.8% of data for which winds were retrieved.
- The bias w.r.t to ERA-5 is 0.22 m/s.; The standard deviation is 1.34 m/s.

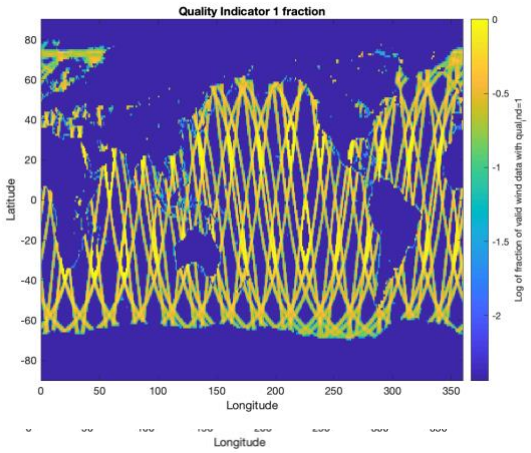

- **Quality Indicator 1** – Insignificantly corrupted retrieval - high quality retrievals; recommended for use is general research
  - This category is like QI=0, except for *it includes only single beam swath data* (i.e. all rain or ice-affected data excluded from quality indicator 0 is also excluded from quality indicator 1.
  - This data set comprises 18.1% of the data with retrieved winds.
  - The bias with respect to ERA-5 is 0.3 m/s. The standard deviation with respect to ERA-5 is 1.76 m/s.

- **Quality Indicator 2** - Possible Significant Error –These are data with rain detected in the cell or in the 7x7 neighbors. Rain correction was applied and it resulted in modifying the speed by <15m/s. Data with QI=2 should be used with caution:
  - **data should be excluded** if rain contamination issues are of importance and the correction to the wind speed applied in rain is deemed questionable;
  - **data should be included** when rain contamination is less important than issues related to missing data in rain (large gaps; excluding data in the most dynamic regions). Several studies have found that excluding rain contaminated data is more detrimental to the accuracy of climatology of wind derivative quantities than including data where large corrections were made.

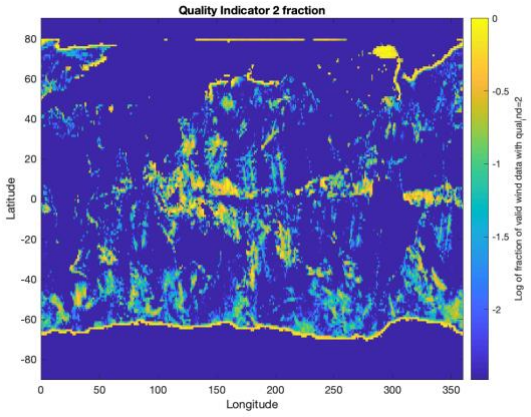

  - Marked with QI=2 are also data with ice in the 7x7 neighborhood but not in the wind vector cell itself.
  - This data set comprises 5.3% of the data with retrieved winds.
  - The bias with respect to ERA-5 is 2.38 m/s. The standard deviation is 6.2 m/s.
    - When latitude is restricted to within + or - 70 degrees. Bias=1.55 m/s; standard deviation=3.4 m/s.

- **Quality Indicator 3** – Likely Significant Error - data should only be used in situations in which data gaps are more problematic than poor quality data. Even then it is recommended to

use the quality flag bits to exclude data with ice or poor coastal retrieval. Ice and poor coastal retrievals occur near the edge of the usable swath and thus do not produce gaps in the data.

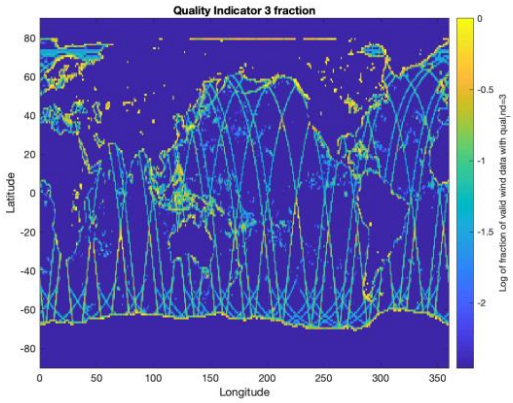

- includes poor coastal retrievals (lake or ocean), rain contamination for which the speed correction was greater than 15 m/s, data with the ice in the wind vector cell, negative and identically zero wind speeds, the outer 3 cross track bins on each side of the swath and the rain-contaminated outer beam only data for which rain contamination is not correctable.
- This comprises 2.76% of the data with wind retrievals. Note that the percentages of Quality indicator 0,1,2, and 3 wind data sum to 100% because winds are not retrieved at all when the quality indicator is 4 or 5.
- The Bias with respect to ERA-5 is 1.97 m/s. The standard deviation is 6.9 m/s.
  - When latitude is restricted to within +- 70 deg. Bias=1.04 m/s; standard deviation=3.4 m/s.

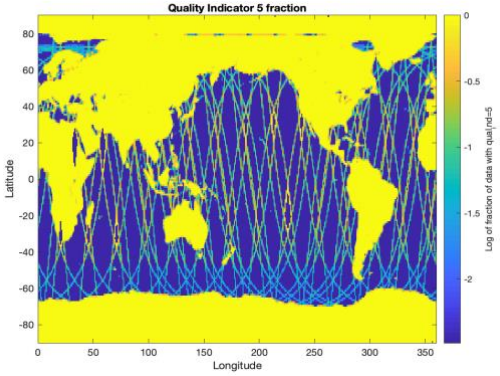

- **Quality Indicator 4** –- No winds retrieved due to quality control
- **Quality Indicator 5** - No data over liquid water in cell -
  - data over land, ice, and swath edges with no sigma-0s, as desired.

Table 1: Comparison vs. ASCAT for various QuikSCAT Quality Index values for 1 year of data

1 year of data and within 30 minutes except as noted	**RMS Speed** (m/s)	**Speed Bias** QuikSCAT-ASCAT (m/s)	**RMS Direction Error** (deg)	**Direction Bias (deg)**	**Number of Samples**
QI 0 ASCAT> 3 m/s	1.114	-0.019	16.6	-0.392	12,247,355
QI 1 ASCAT> 3 m/s	1.243	0.021	16.0	-0.536	3,523,489
QI 2 ASCAT (1 week of data, within 90 minutes)	2.5	0.345			313,636

QI 2 ASCAT>3 m/s	1.837	-0.135	22.1	-0.261	2,210,498
QI 2 ASCAT>3 m/s abs(lat)<70	1.781	-0.155	22.1	-0.615	1,669,439
QI 3 (1 week of data, within 90 minutes)	2.58	0.23			103,541
QI 3 ASCAT>3 m/s	2.102	0.191	22.6	-0.069	664,366
QI3 ASCAT> 3 m/s, abs(lat)<70	2.102	0.228	22.4	-0.37	545,778

4.2.3.2.ASCAT-A/B

The ASCAT Quality indicator is defined the same as for QuikSCAT except:

- the suboptimal portion of the swath is defined differently
- rain contamination, which is much less of a problem for C-band, is currently neither detected nor corrected
- retrieval near the coast is not attempted so the poor coastal correction flag is never set.

- **Quality Indicator 0** - No Retrieval corruption
  - means good part of swath, not on ice edge, and no missing looks.
  - the only difference from the QuikSCAT definition is data too close to the edge of the swath is excluded even if it has no missing looks.
  - 92.4% of data with winds retrieved
  - RMS difference from 37.5-km by 37.5 km mean wind speed is 0.16 m/s.
  - Quality Indicator 1- Insignificantly corrupted retrieval
  - not on or near the ice edge, but can be in suboptimal part of swath or have missing looks.
  - 7.2% of data with winds retrieved
  - RMS difference from 37.5-km by 37.5 km mean wind speed is 0.23 m/s.
- **Quality Indicator 2** - Possible Significant Error
  - same definition as QuikSCAT but because rain contamination is not detected in the ASCAT data set, only data near but not on the ice edge is in this category
  - 1.4% of the data with winds retrieved
  - RMS difference from 37.5-km by 37.5 km mean wind speed is 0.47 m/s.
  - Quality index 3 - Likely Significant Error –
  - Retrievals from observations on the ice edge.
  - 0.4% of the data with winds retrieved
  - RMS difference from 37.5-km by 37.5 km mean wind speed is 0.75 m/s.

Additional evaluations of the quality indicators are presented in the next section on the Uncertainty.

4.2.4. Uncertainty

Our products are providing, for the first time, estimation of the uncertainty for each wind retrieval cell. These estimates are needed while performing detailed analyses of the scatterometer wind retrievals and critically needed when assimilating the wind retrievals into numerical weather prediction models.

Uncertainty estimates were developed by performing triple-collocations among QuikSCAT, ASCAT-A (JPL retrievals with $CMOD7_{adjusted}$, i.e. $CMOD7_{JPL}$), and ERA-5 model first guess (FG) winds (interpolated in space and time to the collocated scatterometer observations). Wind speeds from remote sensors are often validated (and their uncertainty estimated) by comparison with a "ground truth" wind field either from another sensor, a numerical wind product, or buoys. Such a validation suffers from the problem that it is impossible to determine whether differences are errors in the system under test or in the ground truth. The triple collocation technique (Vogelzang et al, 2012; Freilich and Dunbar 1999) uses three data sets and allows random error terms to be estimated for all three. Biases and scaling factors are also determined for two data sets with respect to the third. The technique assumes errors are uncorrelated among the three data sets. We did not include any representation error term. This term is likely small given the similar spatial resolution between QuikSCAT, ASCAT, and ERA5. Wind-retrieval uncertainties for QuikSCAT and ASCAT have been determined from the triple collocation error estimates.

Since scatterometer wind errors vary depending on look geometry and wind speed, we performed this triple colocation analysis as a function of wind speed (for ASCAT and QuikSCAT) and cross-track position (for QuikSCAT). Future versions of this product will estimate errors also as a function of ASCAT cross-track position.

Collocated measurements with an overpass time difference between QuikSCAT and ASCAT-A of +-30 minutes were used. Sensitivity analysis for 60 and 90 minute overpass time differences found minimal sensitivity to time difference, with a small scaling factor >1 for 60 and 90 minute differences. Only data of the highest quality (quality indicator 0 or 1) were used.

Using these techniques, a lookup table was formed for QuikSCAT that estimates EN wind speed and EN wind direction error as a function of wind speed and cross track location. This lookup table was created based on three years of data between 2007-2010. Errors in wind speed and direction were chosen (as opposed to u/v components) to maintain the relationship between cross-track location and speed/direction error, a relationship that does not similarly exist when using components. A similar lookup table was formed for ASCAT that is only a function of wind speed. To estimate errors in u/v wind components, the speed/direction lookup tables are used, with errors propagated through to u/v using standard error propagation formula.

The estimated errors for QuikSCAT are shown in Figure 8. Figure 8, left pane, shows the ratio of wind speed standard deviation to the wind speed, with colors representing wind speed. A cross track index of 0 represents the center of the swath and 70 represents either edge. We find larger wind speed errors along the center and edges of the swath and lower errors in the sweet spots—an expected result given look geometries. As radar SNR improves with increasing wind speed, we expect lower values of $Kp = std(\sigma_o)/\sigma_o$, until around 12 m/s where Kp asymptotes to a constant small value ~0.1 for QuikSCAT and ~0.03 for ASCAT. This asymptotic behavior of Kp is related to the wind speed error by dWS/WS~Kp/alpha, where alpha as approximately 2. Our results for wind speed error are in line with Kp theory and values for QuikSCAT/ASCAT.

Similarly, wind direction errors are shown in Figure 8, right pane. At low wind speeds, the wind direction error is substantially higher, but quickly drops to below 10 degrees at 10 m/s. This is

largely due to the Kp argument above, with low radar SNR at low wind speeds. The wind direction error is highest at the center of the swath, and lowest in the sweet spots around cross track = 50.

We expect significantly larger errors where rain or other radar footprint contamination exists than the estimated ones using triple colocation from quality indicator 0,1 data. Since not enough data exist to perform this analysis stratified by cross track location, wind speed, and quality indicator, we estimate bulk scaling factors between QI=0,1 vs QI=2,3 data, and apply those scaling factors to data where QI=2,3. Figure 9 shows the overall error as a function of quality indicator. QI=2 typically has errors of about twice QI=0,1, and QI=3 about 1.5 times the error of QI=0,1.

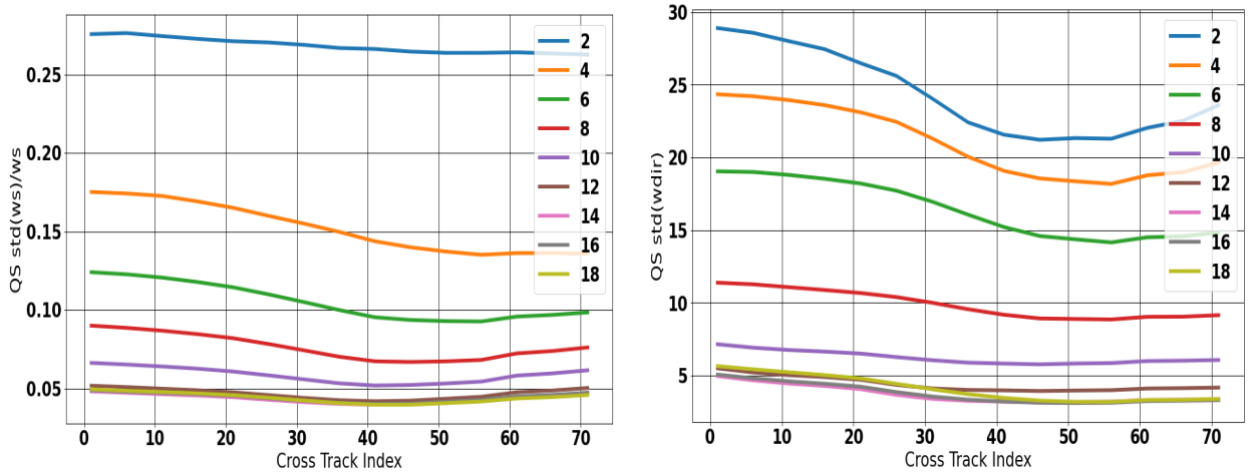

Figure 8. Standard deviation of the QuikSCAT wind speed (left panel) and wind direction (right panel), computed as a function of cross-track position and wind magnitude for several wind regimes. The errors (uncertainties) were computed from triple collocation error analyses of QuikSCAT, ASCAT and ERA-5 EN winds.

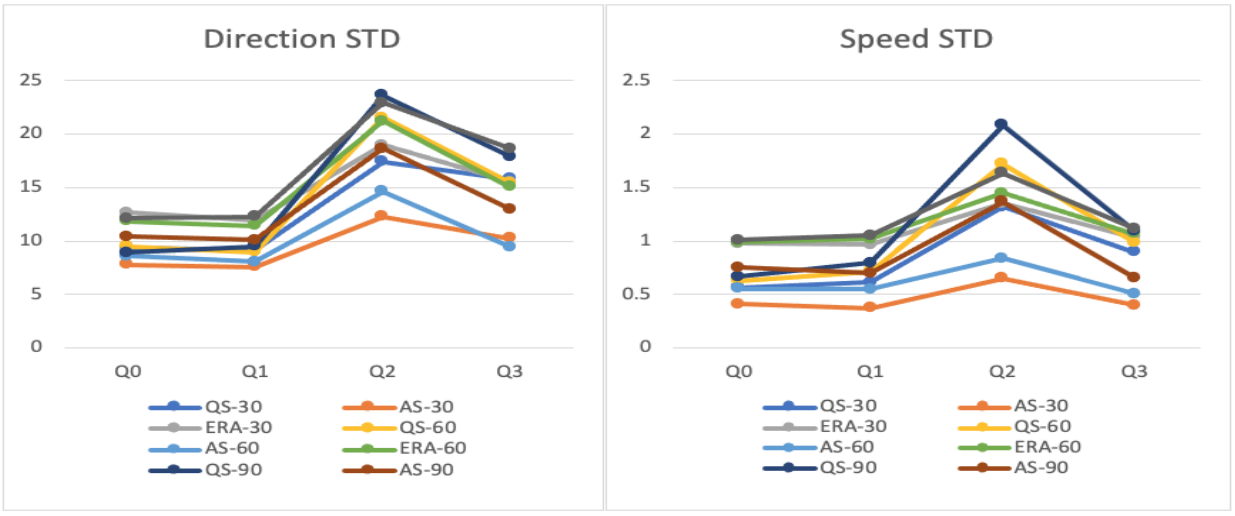

Figure 9. Error statistics as a function of the QuikSCAT Quality Indicator, performed for three sets of QuikSCAT/ASCAT collocations, depending on the time difference between the observations (30 min, 60 min and 90 min)

Figure 9 also shows the sensitivity to triple colocation error to overpass time-difference. As expected, with increasing time differences between QuikSCAT and ASCAT overpasses, the estimated error for measurements goes up; however, a similar trend across quality indicator is observed for all time differences.

From Figure 9, we also observe that ASCAT has the lowest errors compared to QuikSCAT and ERA5. This is not surprising considering the improved viewing geometry and better Kp values associated with ASCAT compared to QuikSCAT. ERA5 has the largest errors compared to the scatterometers.

We performed the same analysis using stress estimates from QuikSCAT, ASCAT-A, and ERA5 to provide an estimate of the wind stress ***magnitude*** error. Because the EN wind direction and the wind stress direction are the same, the errors in wind stress direction are the same as EN wind direction errors.

We have not performed this analysis using the true wind products; these errors, while provided, are duplicates of the EN wind errors. We do not expect a significant difference between estimated EN wind errors and true wind errors.

Results for one day of QuikSCAT data are shown in Figure 10, with wind speed errors on the left and wind direction errors on the right. In areas where QI=2,3 are set, the base error in wind speed/direction are multiplied by scaling factors as detailed above. This is clear in rainy areas, where large errors are observed due to set quality indicators. Similarly, increased errors are observed along ice edges due to set ice quality indicators. Along the center of the swath, errors are also clearly increased, consistent with Figure 8. Not as apparent in Figure 10 are the increased errors at low wind speeds, which become clear when comparing to a global map of wind speed.

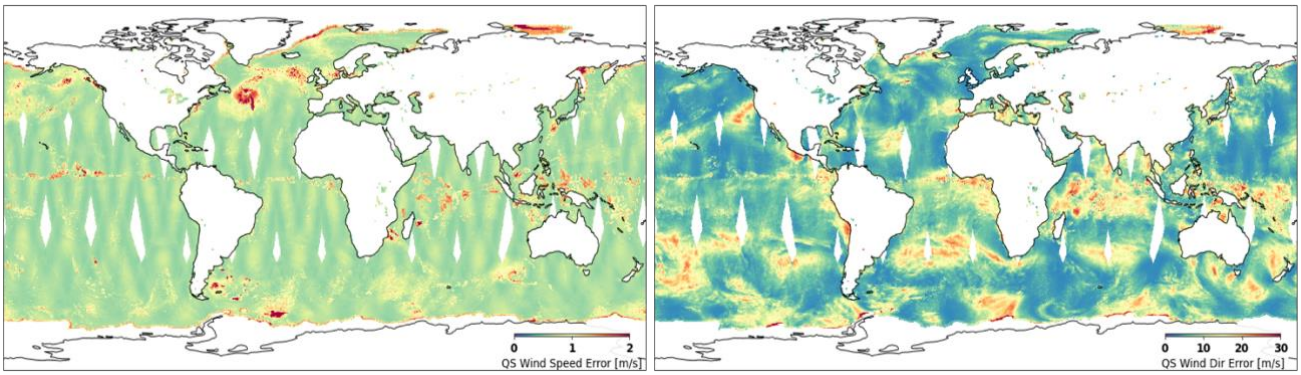

Figure 10. Illustration of the uncertainty, as determined from 1 day of QuikSCAT observations. Left panel shows the uncertainty in the speed estimations while the right panel show the uncertainty in the direction estimations.

5. Results from evaluations so far

5.1. Evaluation of the Level 2 Type A products using buoy data.

Evaluating the performance of our retrievals against buoy observations has been a major focus of our recent work.

5.1.1. Understanding the quality of the buoy data

We began this effort by looking into the buoy wind speed error. The relative accuracy of buoy winds with extreme sea states was quantified through a triple collocation exercise comparing buoy winds to winds from ASCAT (KNMI retrievals) and ERA5 First Guess winds. The results from this analysis are shown in Wright et al. (2021) and are summarized here.

Differences between buoy winds and ASCAT were analyzed through separating the residuals by anemometer height and testing under high wind-wave and swell conditions. First, we convert buoy winds measured at 3, 4 and 5 m to stress-equivalent and winds at 10 m (U10S) using the COARE 3.5 algorithm with a wind only formulation for roughness length. We found that the availability of high winds collocations from buoys with anemometers near 3m were severely limited as most of these buoys are located in tropical regions. Using triple collocation calibration of buoy U10S to ASCAT in pure wind-wave conditions defined by the ERA5/ECMWF wave model (Bidlot 2018), we find that there is a small, but statistically significant difference between height adjusted buoy winds from buoys with 4 and 5 m anemometers compared to the same ASCAT wind speed ranges in high seas. However, this result does not follow conventional arguments for wave sheltering of buoy winds, whereby the lower anemometer height winds are distorted more than the higher anemometer height winds in high winds and high seas. On average, calibrated buoy U10S from buoys with anemometers near 4 m compared slightly higher than buoys with anemometers near 5 m in wind-wave conditions with significant wave height between 4 and 5 m and wind speeds between 12 and 18 m/s (Figure 11). From these results we concluded that errors from flow distortion of the waves on buoy winds are not a dominant factor on buoy wind speed error for buoys with anemometers near 4 and 5 m, with high confidence in our results for winds below 18 ms^{-1}. Further evaluation of buoys with lower anemometer heights is needed as more observations in high winds become available.

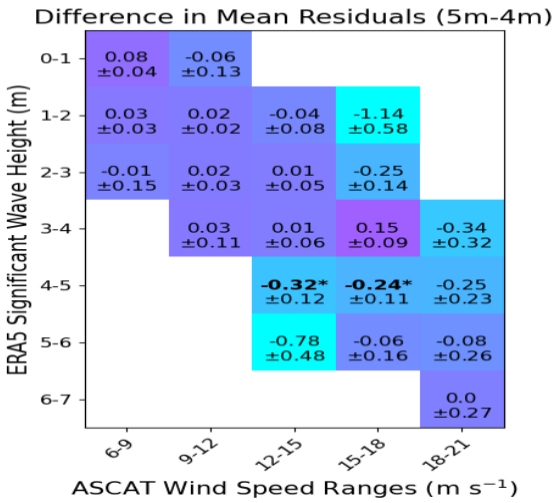

Figure 11. Heat map of the difference between the binned average of calibrated wind speed residuals (calibrated buoy U10S–ASCAT) for ASCAT wind and ERA5 H_s ranges for buoy residuals at 5 m minus the binned residuals at 4 m anemometer height in wind-wave-dominated seas. Bold values with an asterisk (*) indicate statistically significant differences between the residuals at separate anemometer heights defined using Welch's t–test with a p–value limit of 0.05.

5.1.2. NDBC Buoy observations as a source of the truth: Comparisons of scatterometer retrievals to buoy data

In this work we took advantage of the NDBC Buoy measurements to quantitatively characterize and validate the four scatterometer-derived ocean surface wind products: ASCAT-$A_{KNMI\text{-}CMOD7}$, ASCAT-$A_{JPL\text{-}CMOD7}$, ASCAT-$A_{JPL\text{-}CMOD7jpl}$, and QuikSCAT$_{JPL\text{-}KuSST}$ for the year 2008. The retrieved winds compared fairly well with buoys in the presence of QC-flags (the lower panel Fig. 12 & Table 2), though at low and high wind speeds scatterometer measurements may be somewhat affected. The overall ASCAT-A initial comparison indicates a very slight improvement in wind speed quality going from the KNMI original ASCAT-A to JPL processed ASCAT-A data. The JPL QuikSCAT

retrievals compare very slightly better in the mean bias but have larger RMSD and standard deviation compared to the ASCAT comparisons to the buoy (Table 2). These results support the validity of our approach. Future plans involve continued use of the buoys for validation, with considerations to examine impacts from tropical rain/convection including the recently available ScatSat retrieved data.

Note: the differences between the three ASCAT-A products are minuscule. What is more important is that the ASCAT-A$_{JPL\text{-}CMOD7jpl}$ retrievals maintain their quality with respect to buoy, while at the same time provide wind retrievals that are consistent with QuikSCAT's as illustrated by Figures 1, 2 and 3 in Sec 4.1. Indeed, this has been our goal.

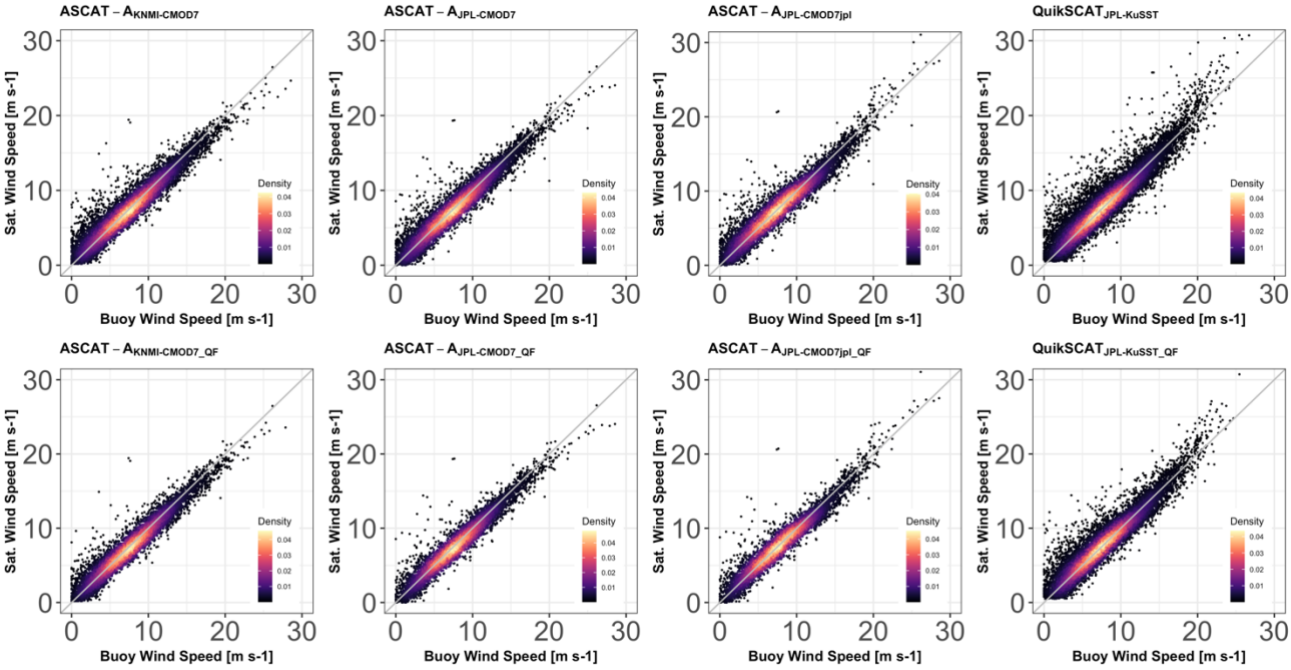

Figure 12. 2D-density plot of collocated scatterometer (Sat.) winds against NDBC buoy wind speeds for the year 2008. The diagonal gray line is the 1:1 agreement. Quality Control (title with suffix QF as shown in the lower panel figure) flags were applied by discarding any records that were flagged as fatal or poor quality (see the QC-flags header description in the data).

Table 2. Validation (scatterometer vs. buoy) summary. The statistical parameters RMSD, μ, σ, ρ, and N are the root mean square difference, mean difference (scatterometer - buoy), standard deviation of the difference, correlation between scatterometer & buoy, and the total sample size of the collocated scatterometer and buoy wind data, respectively. The suffix QF at the end of the scatetterometer title indicates quality control flags were applied.

Scatterometer	N	μ m s^{-1}	RMSD m s^{-1}	σ m s^{-1}	ρ
ASCAT-A$_{KNMI\text{-}CMOD7}$	14228	-0.04	1.07	1.07	0.96
ASCAT-A$_{KNMI\text{-}CMOD7_QF}$	11507	-0.13	0.95	0.94	0.97
ASCAT-A$_{JPL\text{-}CMOD7}$	12063	-0.10	1.04	1.03	0.96
ASCAT-A$_{JPL\text{-}CMOD7_QF}$	8718	-0.16	0.95	0.93	0.97
ASCAT-A$_{JPL\text{-}CMOD7jpl}$	12064	-0.02	1.05	1.05	0.96
ASCAT-A$_{JPL\text{-}CMOD7jpl_QF}$	8719	-0.08	0.95	0.95	0.97
QuikSCAT$_{JPL\text{-}KuSST}$	25068	0.10	1.25	1.25	0.94
QuikSCAT$_{JPL\text{-}KuSST_QF}$	18887	0.06	1.14	1.13	0.95

6. What is in this set if delivered products

- L2 products scatterometer retrievals of wind and stress from
  - QuikSCAT and ASCAT-A during the period of tandem observations (2007-2009)
  - ScatSat and ASCAT-B retrieval from the period of tandem operations (2018-2019)
- L2 ancillary data:

For each of the scatterometer data records above, collocated in space and time wind/stress data from ERA-5 (including SST, surface pressure, 2m temperature and relative humidity), surface precipitation from IMERG, and the surface currents from GlobeCurrents.

7. What is coming next in the near term

- Derivatives of the wind and the stress from the periods of tandem operations between QuikSCAT and ASCAT-A and ScatSat and ASCAT-B
- Level 3 products of all existing L2 products
- Modifications in response to user's comments
- Processing of the entire record

8. Acknowledgments

Our project could not have gone forward without the great support we received from Stefanie Linow (Stefanie.Linow@eumetsat.int) and Debbie Richards, both from EUMETSAT. We really appreciate their critical help in providing us with the L1B SZF data in the native format (not HDF), containing the full resolution sigma0sigma0 observations. These were the CDR for ASCAT-A and GDS for ASCAT-B/C.

References:

Atlas, R., and Coauthors, 2001: The effects of marine winds from scatterometer data on weather analysis and forecasting. *Bull. Amer. Meteor. Soc.*, **82**, 1965–1990, https://doi.org/10.1175/1520-0477(2001)082<1965:TEOMWF>2.3.CO;2.

Bhate, J., Munsi, A., Kesarkar, A., Kutty, G., & Deb, S. K., 2021: Impact of assimilation of satellite retrieved ocean surface winds on the tropical cyclone simulations over the north Indian Ocean. Earth and Space Science, 8, e2020EA001517. https://doi.org/10.1029/2020EA001517

Bidlot, J.-R., 2018: *Part VII: ECMWF Wave-Model Documentation*; IFS Documentation Cycle CY23R4; ECMWF: Reading, UK

Bourassa, M. A., H. Bonekamp, P. Chang, D. Chelton, J. Courtney, R. Edson, J. Figa, Y. He, H. Hersbach, K. Hilburn, T. Lee, W. T. Liu, D. Long, K. Kelly, R. Knabb, E. Lindstorm, W. Perrie, M. Portabella, M. Powell, E. Rodriguez, D. Smith, A. Stoffelen, V. Swail, and F. Wentz, 2010: Remotely sensed winds and wind stresses for marine forecasting and ocean modeling. *Proceedings of the OceanObs'09: Sustained Ocean Observations and Information for Society Conference (Vol. 2)*, Venice, Italy, eds. J. Hall, D.E. Harrison and D. Stammer, ESA Publication WPP-306. doi:10.5270/OceanObs09.cwp.08

Bourassa, M. A., Rodriguez, E., and Gaston, R. (2009). Summary of the 2008 NASA ocean vector winds science team meeting. *Bull. Am. Meteorol. Soc*. 91, 925–928. doi: 10.1175/2010BAMS2880.1

Bourassa, M.A. 2006. Satellite-based observations of surface turbulent stress during severe weather. Pp. 35–52 in Atmosphere- Ocean Interactions, vol. 2. W. Perrie, ed.,Wessex Institute of Technology Press, Southampton, UK.

Chavas, D. R., and K. A. Emanuel, 2010: A QuikSCAT climatology of tropical cyclone size. *Geophys. Res. Lett.*, **37**, L18816, doi:10.1029/2010GL044558

Chelton, D. B., M. G. Schlax, M. H. Freilich, and R. F. Milliff, 2004: Satellite measurements reveal persistent small-scale features in ocean winds. Science, 303, 978-983.

Cunningham et al., 2007

Drennan, W. M., P. K. Taylor, and M. J. Yelland, 2005: Parameterizing the sea surface roughness. J. Phys. Oceanogr., 35, 835–848.

Edson, J. B., V. Jampana, R. A. Weller, S. Bigorre, A. J. Plueddemann, C. W. Fairall, S. D. Miller, L. Mahrt, D. Vickers, and H. Hersbach, 2013: On the exchange of momentum over the open ocean. J. Phys. Oceanogr., 43, 1589–1610.

Freilich, M. H., and R. S. Dunbar,1999: The accuracy of the NSCAT 1 vector winds: Comparisons with National Data Buoy Center buoys, J. Geophys. Res., 104(C5), 11231–11246, doi:10.1029/1998JC900091

Gierach, M. M.,, M. A. Bourassa, P. Cunningham, J. J. O'Brien, and P. D. Reasor, "Vorticity-based detection of tropical cyclogenesis," *J. Appl. Meteorol. Climatol.*, vol. 46, pp. 1214–1229, Aug. 2007, doi: 10.1175/JAM2522.1.

GPM Integrated Multi-Satellite Retrievals for GPM (IMERG) Algorithm Theoretical Basis Document (ATBD) v5.2 - https://gpm.nasa.gov/resources/documents/gpm-integrated-multi-satellite-retrievals-gpm-imerg-algorithm-theoretical-basis-

Hristova-Veleva, S.M.; Rodriguez, E.; Haddad, Z.; Stiles, B.; Turk, F.J., "Hadley cell trends and variability as determined from scatterometer observations: How RapidScat will help establishing reliable long-term record," in *Geoscience and Remote Sensing Symposium (IGARSS), 2015 IEEE International* , vol., no., pp.1211-1214, 26-31 July 2015, doi: 10.1109/IGARSS.2015.7325990 URL: http://ieeexplore.ieee.org/stamp/stamp.jsp?tp=&arnumber=7325990&isnumber=7325670

Hristova-Veleva, S. M., Z. S. Haddad, B. W. Stiles, T. P. J. Shen, N. Niamsuwan, F. J. Turk, P. P. Li, B. W. Knosp, Q. A. Vu, B. H. Lambrigtsen, and W. L. Poulsen, 2016a: Possible predictors for the rapid intensification and evolution of hurricanes from near-coincident satellite observations of the structure of precipitation and surface winds: Hurricane Joaquin, *32nd AMS Conference on Hurricanes and Tropical Meteorology*, San Juan, PR https://ams.confex.com/ams/32Hurr/webprogram/Paper293955.html

Hristova-Veleva, S. M., T. Lee, B. Stiles, E. Rodriguez, F. J. Turk, Z. Haddad, 2016: The 2015-16 El Niño - birth, evolution and teleconnections from scatterometer observations of the ocean surface winds, *EUMETSAT*, Darmstadt, Germany, September 2016b, https://www.eumetsat.int/website/home/News/ConferencesandEvents/DAT_2833302.html

Hristova-Veleva, S., Z. Haddad, B. Stiles, 2016c: "Accurate estimation of the ocean surface winds in hurricanes – a critical component for developing predictors for hurricane Rapid Intensification potential", International workshop on measuring high-wind speeds over the ocean, 15-17 November 2016, Met Office, Exeter

Isaksen, L., and Stoffelen, A. (2000). ERS scatterometer wind data impact on ECMWF's tropical cyclone forecasts. *IEEE Transactions on Geoscience and Remote Sensing*, **38**(4), 1885–1892.

Jiang et al., 2008

Kara, A. B., A. J. Wallcraft, and M. A. Bourassa, 2008: Air-Sea Stability Effects on the 10m Winds Over the Global Ocean: Evaluations of Air-Sea Flux Algorithms. *J. Geophys. Res*., **113**, C04009, doi:10.1029/2007JC004324.

Kilpatrick, T., & Xie, S.-P., 2015: ASCAT observations of downdrafts from mesoscale convective systems.Geophysical Research Letters,42,1951–1958. https://doi.org/10.1002/2015GL063025

Kloe, J. de, A. Stoffelen, and A. Verhoef, 2017: Improved use of scatterometer measurements by using stress-equivalent reference winds. IEEE J. Sel. Top. Appl. Earth Obs. Remote Sens., 10(5), doi:10.1109/JSTARS.2017.2685242.

King, G. P., et al., 2022, Correlating Extremes in Wind Divergence with Extremes in Rain over the Tropical Atlantic, *Remote Sens.* **2022**, *14*(5), 1147; https://doi.org/10.3390/rs14051147

Kudryavtsev, V. N., and V. K. Makin, 2001: The impact of the air flow separation on the drag of the sea surface, Boundary Layer Meteorol., 98, 155–171.

Large, W. G., J. C. McWilliams. and S. C. Doney, 1994: Oceanic vertical mixing: A review and a model with nonlocal boundary layer parameterization. Rev. Geophys., 32, 363-403.

Liu, W. T. and W. Tang, (1996). *Equivalent Neutral Wind*. JPL Publication 96-17, Jet Propulsion Laboratory, Pasadena, 16 pp.

Lovenduski, N. S., and N. Gruber, 2005, Impact of the Southern AnnularMode on Southern Ocean circulation and biology,Geophys. Res. Lett.,32, L11603, doi:10.1029/2005GL022727.

McCarty, W., Chattopadhyay, M., & Conaty, A. (2018). Evaluation of RapidScat ocean vector winds for data assimilation and reanalysis. *Monthly Weather Review*, **146**(1), 199–211

Marseille, G.-J., and Stoffelen, A. (2017). Toward scatterometer winds assimilation in the mesoscale HARMONIE Model. *IEEE Journal of Selected Topics in Applied Earth Observations and Remote Sensing*, **10**(5), 2383–2393.

Minobe, S., A. Kuwano-Yoshida, N. Komori, S.-P. Xie, and R. J. Small, 2008: Influence of the Gulf Stream on the troposphere. Nature, 452, 206–209.

O'Neill, L. W., D. B. Chelton, S. K. Esbensen, and F. J. Wentz, 2005: High-resolution satellite measurements of the atmospheric boundary layer response to SST perturbations over the Agulhas Return Current. J. Climate, 18, 2706–2723.

Ricciardulli, L. and F. J. Wentz, "A scatterometer geophysical model function for climate-quality winds: QuikSCAT Ku-2011," J. Atmospheric Ocean. Technol., vol. 32, pp. 1829–1846, 2015.

Ricciardulli, L., 2016: "ASCAT on Metop-A Data product update notes: V2.1 data release," Remote Sensing Systems, Santa Rosa, CA, USA, Tech. Rep. 040416.

Ricciardulli and Wentz, OVWST presentation, 2017

Ricciardulli, L., and A. Manaster, 2021: "Intercalibration of ASCAT Scatterometer winds from MetOp-A, -B, and -C, for a Stable Climate Data Record", *Remote Sensing.* 13(18), 3678. https://doi.org/10.3390/rs13183678

Rio M-H, Mulet S, Picot N. Beyond GOCE for the ocean circulation estimate: Synergetic use of altimetry, gravimetry, and in situ data provides new insight into geostrophic and Ekman currents. Geophysical Research Letters [Internet]. Wiley-Blackwell; 2014 Dec 18;41(24):8918–25. Available from: http://dx.doi.org/10.1002/2014gl061773

Ross, D.B., V.J. Cardone, J. Overland, R. D. McPherson, W. J. Pierson Jr., and T. Yu, (1985). Oceanic surface winds. *Adv. Geophys*., **27**, 101–138.

SeaPAC. 2020. QuikSCAT Level 2B Ocean Wind Vectors in 12.5km Slice Composites Version 4.1. Ver. 4.1. PO.DAAC, CA, USA. Dataset accessed [2022-01-02] at https://doi.org/10.5067/QSX12-L2B41

Stoffelen et al, IEEE JSTARS 2017

Suzuki, N., T. Hara, and P. P. Sullivan, 2013: Impact of breaking wave form drag on nearsurface turbulence and drag coefficient over young seas at high winds. J. Phys. Oceanogr. 43, 324-343.

Verhoef, A., J. Vogelzang, J. Verspeek, and A. Stoffelen, 2017: Long-term scatterometer wind climate data records," IEEE J. Sel. Topics Appl. Earth Observ. Remote Sens., vol. 10, no. 5, pp. 2186–2194, May 2017, doi:10.1109/JSTARS.2016.2615873

Vogelzang, J. and A. Stoffelen, 2012: NWP Model Error Structure Functions Obtained From Scatterometer Winds. *IEEE Trans. Geosci. Remote Sensing*, *50*(7), 2525–2533, doi:10.1109/TGRS.2011.2168407.

Wang Z., *et al*., "SST Dependence of Ku- and C-Band Backscatter Measurements," in *IEEE Journal of Selected Topics in Applied Earth Observations and Remote Sensing*, vol. 10, no. 5, pp. 2135-2146, May 2017, doi: 10.1109/JSTARS.2016.2600749.

Wentz, F., Ricciardulli, L., Rodriguez, E., Stiles, B., Bourassa, M., Long, D., et al., 2017: Evaluating and extending the ocean wind climate data record. *IEEE J. Sel. Top. Appl. Earth Observ. Remote Sens.* 10, 2165–2185. doi: 10.1109/JSTARS.2016.2643641

Wright, Ethan E., Mark A. Bourassa, Ad Stoffelen, and Jean-Raymond Bidlot, 2021: "Characterizing Buoy Wind Speed Error in High Winds and Varying Sea State with ASCAT and ERA5." Remote Sensing 13, no. 22: 4558.